

See discussions, stats, and author profiles for this publication at: <https://www.researchgate.net/publication/51557550>

# In Situ Recording of Particle Network Formation in Liquids by Ion Conductivity Measurements

ARTICLE *in* JOURNAL OF THE AMERICAN CHEMICAL SOCIETY · AUGUST 2011

Impact Factor: 12.11 · DOI: 10.1021/ja205287d · Source: PubMed

CITATIONS

10

READS

29

7 AUTHORS, INCLUDING:



**Christian Pfaffenhuber**

Max Planck Institute for Solid State Research

6 PUBLICATIONS 38 CITATIONS

SEE PROFILE



**Marjan Bele**

National Institute of Chemistry

100 PUBLICATIONS 2,512 CITATIONS

SEE PROFILE



**Marcus Constantin Göbel**

Heraeus Holding

11 PUBLICATIONS 92 CITATIONS

SEE PROFILE


# In Situ Recording of Particle Network Formation in Liquids by Ion Conductivity Measurements

Christian Pfaffenhuber,<sup>†</sup> Seniz Sörgel,<sup>†</sup> Katja Weichert,<sup>†</sup> Marjan Bele,<sup>§</sup> Tabea Mundinger,<sup>‡</sup> Marcus Göbel,<sup>†</sup> and Joachim Maier<sup>\*,†</sup>

<sup>†</sup>Max Planck Institute for Solid State Research, D-70569 Stuttgart, Germany

<sup>‡</sup>Max-Planck-Institute for Intelligent Systems, D-70569 Stuttgart, Germany

<sup>§</sup>National Institute of Chemistry Slovenia, 1000 Ljubljana, Slovenia

 Supporting Information

**ABSTRACT:** The formation of fractal silica networks from a colloidal initial state was followed in situ by ion conductivity measurements. The underlying effect is a high interfacial lithium ion conductivity arising when silica particles are brought into contact with Li salt-containing liquid electrolytes. The experimental results were modeled using Monte Carlo simulations and tested using confocal fluorescence laser microscopy and  $\zeta$ -potential measurements.

Aggregation of solid particles dispersed in solvents is a process of great technological significance. The range of applications is very wide, covering such diverse issues such as dispersion paints,<sup>1</sup> catalysts,<sup>2</sup> and electrolytes.<sup>3</sup> While colloids are stabilized by electrostatic repulsion or interaction with the solvent, short-ranged solid–solid interactions, usually van der Waals interactions, always drive aggregation.

Particularly clear is the situation with lyophobic colloids. Here the particles are separated by electrostatic repulsion of alike surface charges. Upon collision, however, with electrostatic repulsion providing an activation threshold, particles hit and stick together because of the stronger short-range interactions (van der Waals or even covalent bonding). As a result of these interactions, larger and larger aggregates form by cluster–cluster aggregation. If the hit-and-stick mechanism is essentially irreversible and faster than the coarsening kinetics, fractal networks form.

Particle dispersions of oxides in liquids have recently become important for Li-based batteries as a novel class of semisolid electrolytes with high Li ion transference numbers (“soggy sand electrolytes”).<sup>4</sup> In this class of materials, insulating inorganic particles admixed with salt-containing liquid electrolytes lead to greatly improved mechanical and electrical properties. Typical examples are LiClO<sub>4</sub>-containing polyethylene glycol (PEG) electrolytes to which fine SiO<sub>2</sub> particles have been added. These systems have been investigated experimentally (mostly in the context of ionic conductivity) as well as by the use of purely statistical simulations.<sup>5–7</sup>

As a consequence of preferential anion adsorption, ion pairs are broken in the space-charge zones surrounding the particles. Hence, locally the Li<sup>+</sup> transference number and the Li ion conductivity are increased while the anion conductivity is decreased. The resulting mechanical properties resemble those of soft solids in terms of shapeability but are still compatible with nanotechnology because the liquid part of these composites can penetrate into the nanostructured electrolyte networks.

Naturally, a locally enhanced ion conductivity ( $\sigma$ ) is only a necessary condition for improved electrolyte function. What is required for long-range transport is the formation of percolating clusters.<sup>8,9</sup> The volume fraction ( $\varphi$ ) of the second phase should however not be so large that blocking effects occur. They can be observed at high volume fractions and are due to interruption of current paths by nonactive particles or particle aggregates, as observed in many composite electrolytes.<sup>5</sup> This is the reason for typically observed dome-shaped  $\sigma(\varphi)$  characteristics. Recently, extensive modeling of the local mechanism, the formation of fractal networks, and their stability has been performed.<sup>6,10</sup> Numerous studies in the literature [e.g., using confocal fluorescence microscopy (CFM), rheology, and modeling] are concerned with properties or morphologies of such aggregates.<sup>11–14</sup> Additionally, dynamic light scattering (DLS) has often been used to study network formation.<sup>15,16</sup> In these systems, nanoparticles have positive effects on electrical properties even at low  $\varphi$ . In the present contribution, for the first time, the kinetics of aggregate formation were indeed followed in situ by measurements of the ion conductivity. We complemented our studies using CFM and  $\zeta$ -potential experiments as well as combined Monte Carlo simulations and finite element modeling (FEM).

As network formation is crucial to all fields where gels are important, we are convinced that these findings are of general relevance for colloid chemistry and nanotechnology beyond the sheer aspect of arriving at improved Li electrolytes.

Unlike our previous experiments,<sup>5</sup> where we used SiO<sub>2</sub> volume fractions [ $\varphi(\text{SiO}_2)$ ] of  $\geq 1\%$  and hence observed almost immediate formation of macroscopic clusters, leading to a maximum and a subsequent steep decrease of  $\sigma(\varphi)$ , here we used very small  $\varphi(\text{SiO}_2)$  values [ $0.075\% \leq \varphi(\text{SiO}_2) \leq 0.3\%$ ]. With the assumption that the hit rate, and for sufficiently strong interactions also the hit-and-stick rate, are proportional to the product of the number density of the two collision partners, it is clear that the growth kinetics of the fractal clusters sensitively depends on  $\varphi(\text{SiO}_2)$ . Gelation does not necessarily imply fractal networks.<sup>17</sup> In spite of the smallness of  $\varphi(\text{SiO}_2)$ , percolating clusters can be formed provided the particle size is in the nanometer range. This is immediately clear from two simple arguments: (i) The mean distance  $\bar{d}$  between adjacent silica particles of radius  $r$  in the initial colloidal dispersion is  $\bar{d} = 2r/\varphi^{1/3}$

Received: June 8, 2011

Published: August 10, 2011

(i.e., for  $r = 5$  nm and a volume fraction of 0.1%,  $\bar{d}$  is only 100 nm).<sup>18</sup> Hence, the distance between the particles is very small, which in combination with the low mass gives rise to a great encounter probability. (ii) As far as the percolation is concerned, the critical volume fraction at which a singly percolating cluster forms ( $\varphi_c$ ) is proportional to the volume fraction, which scales with a dimensionality of 3, as well as to the reciprocal of the number of particles in that cluster, which scales with the Hausdorff dimensionality. As the latter is smaller than 3,  $\varphi_c$  tends to zero for  $r \rightarrow 0$ .<sup>19</sup>

The composite electrolytes contained vacuum-dried nano-sized SiO<sub>2</sub> [Sigma-Aldrich; 300 nm stated particle diameter, 210 nm actual particle diameter as measured by scanning electron microscopy (SEM) (see Figure S1 in the Supporting Information)] that was dispersed in a 0.1 M solution of LiClO<sub>4</sub> (99.99%, Sigma-Aldrich) or LiOTf (OTf = OSO<sub>3</sub>CH<sub>3</sub>) (99.995%, Sigma-Aldrich) in water-free tetrahydrofuran (THF, 99.9%, unstabilized, Alfa Chemicals). The volume fraction  $\varphi$ -(SiO<sub>2</sub>) was 0.075–0.3%. Ionic conductivities were determined at 25 °C using impedance spectroscopy (Solatron 1260; frequency range, 10<sup>7</sup>–10<sup>−1</sup> Hz; amplitude of oscillating voltage, 0.1 V) by sandwiching the composite electrolytes between two gold-plated electrodes in a custom-built gas-tight cell. The conductivity was evaluated from the intercept of the low-frequency spike with the real axis (see Figure S2), indicating increased surface conduction as the clusters grow.  $\zeta$ -Potential measurements were performed according to the electroacoustic technique using Acoustophor DT-1201 (Dispersion Technology Inc.) in a custom-built gas-tight vessel at room temperature. The dispersion was stirred and sonicated prior to the measurement to separate the particles. CFM images were taken using SiO<sub>2</sub> particles sensitized with a rhodamine 6G dye that was embedded into an additional SiO<sub>2</sub> coating.<sup>18</sup> The only difference was the lower amount of tetraethylorthosilicate used to synthesize smaller particles. Therefore, the physical properties and the agglomeration of the particles were hardly affected by the dye molecules. The images were recorded with an inverted AxioVert 200 M microscope (Zeiss). The fluorescence of the particles was stimulated with a Xe lamp and a no. 38 eGFP filter (Zeiss) with an excitation wavelength of 470 ± 40 nm, an emission wavelength of 525 ± 50 nm, and a beamsplitter at 495 nm. The signals were detected with a 63× C-Apochromat 63×/1.20 W Korr UV–vis–IR object lens (Zeiss) and an ORCA-ER CCD camera (Hamamatsu).

The experiments were modeled using Monte Carlo simulations that took into account the specific interactions of the components in the composite electrolyte, namely, attractive forces between particles and interparticle repulsion stemming from the influence of the solvent and the ions.<sup>20–22</sup> With the help of FEM calculations processed with COMSOL Multiphysics, the local conductivity distribution was calculated for any given structure of the cluster that was formed. A detailed description of the simulations and further results will be given in a forthcoming publication.

Figure 1 shows that  $\sigma$  increased with time for very small  $\varphi$ (SiO<sub>2</sub>), indicating network formation. Since the electrolyte conductivity was not negligible, the measured overall conductivity then increased upon agglomeration even before a percolating cluster was formed. The overall value is thus a complicated function of time and, as far as the theoretical description is concerned, only accessible numerically (see below).

While the network formation kinetics must be a strong function of  $\varphi$ (SiO<sub>2</sub>), this is not the case for the coarsening of the network, which according to our previous considerations<sup>5</sup>

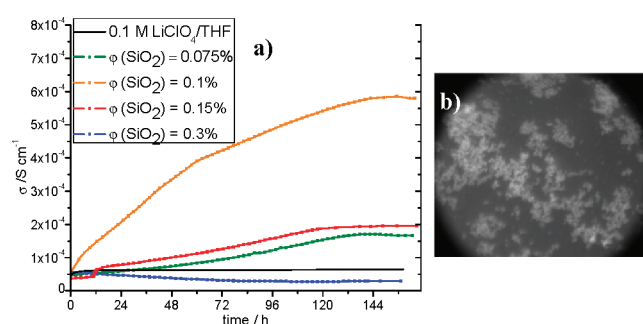


**Figure 1.** (a) Time-dependent ion conductivity of 0.1 M LiClO<sub>4</sub>/THF as a function of SiO<sub>2</sub> volume fraction. (b) CFM image of 0.1 M LiClO<sub>4</sub>/2,2,3,3-tetramethyl-THF/dye-sensitized SiO<sub>2</sub> (particle size 300 nm) with  $\varphi$ (SiO<sub>2</sub>) = 0.15% after 3 days. The total image width is 142  $\mu$ m.

exhibits a typical time constant of  $\sim 1$  h. Hence, we had to reckon with a superposition of network formation and coarsening. As the first leads to an increase in  $\sigma$  while the second decreases  $\sigma$ , this resulted in a flattening at  $\sim 150$  h for  $\varphi$  values of  $\sim 0.1\%$  (see the curves for 0.075, 0.1, and 0.15% in Figure 1a).

The curves for 0.075, 0.10, and 0.15% show the expected maximum due to the counteracting processes of network formation and coarsening. It is a general observation in our experiments that the maximum of conductivity tends to appear earlier with increasing volume fraction (0.1 and 0.15%). This is expected because unlike coarsening, the formation kinetics increases with  $\varphi$ .<sup>5</sup> For 0.3%, the network formation is so fast that only the coarsening kinetics can be observed, and the  $\sigma$  curve monotonically decreases. This is the behavior usually seen in the soggy sand electrolytes.<sup>5</sup> This coarsening is self-decelerating and comes to a kinetic standstill.<sup>5</sup>

The magnitude of the enhancement agrees with the typical dome-shaped  $\sigma(\varphi)$  functionality (increase due to the increased proportion of surface conduction at low  $\varphi$  and decrease due to formation of blocking morphologies at high  $\varphi$ ).<sup>6</sup> The effect of a conductivity increase at low  $\varphi$  is also significantly dependent on the type of solvent. Only in nonpolar systems is the diffusive layer around the particles expanded as a result of the low charge carrier concentration in the composite electrolyte. Here the overlap of double layers is very probable and can be found already at volume fractions of 0.04%.<sup>23</sup>

An elegant way to observe the particle agglomeration as well as the network formation directly is the use of CFM. This technique is able to detect the topology of fluorescent particles in liquids and record agglomeration.<sup>11,14</sup> For this purpose, dye-sensitized SiO<sub>2</sub> particles (diameter  $\sim 300$  nm) were employed. Instead of THF, 2,2,3,3-tetramethyl-THF was used to avoid evaporation of the solvent over the several days of measurement. Apart from a higher boiling point ( $T_b = 121$  °C), 2,2,3,3-tetramethyl-THF has a similar structure and similar dielectric constant ( $\epsilon = 5.1$ ).<sup>24</sup> The conductivity behavior of a 0.1 M LiClO<sub>4</sub>/2,2,3,3-tetramethyl-THF/dye–SiO<sub>2</sub> composite electrolyte was very similar to that of composite electrolytes containing THF (see the Supporting Information). This demonstrates that neither the different solvent nor the SiO<sub>2</sub> modification by the dye significantly changes the mechanism of conductivity increase. Detailed investigations concerning the aggregation kinetics on different kinds of dye-sensitized SiO<sub>2</sub> nanoparticles in the context of the soggy sand electrolytes will be reported in an upcoming paper. Here it suffices to state that the time dependence of the progress

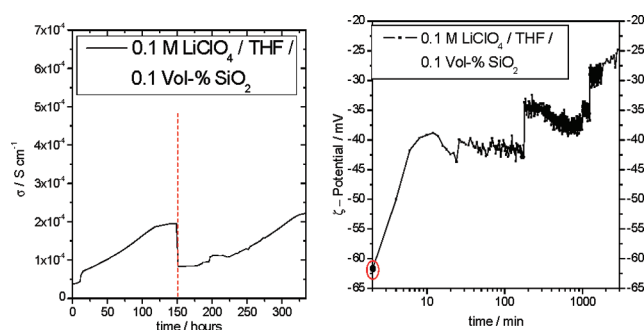


**Figure 2.** a. Time dependent conductivity in 0.1 M LiClO<sub>4</sub>/THF ( $\phi(\text{SiO}_2) = 0.1\%$ ) in combination with ultrasonic treatment (pulses of low intensity with frequency of 0.2 Hz for 1 min) in between (dashed line). b. Time dependent  $\zeta$ -potential of 0.1 M LiClO<sub>4</sub>/THF/SiO<sub>2</sub> ( $\phi(\text{SiO}_2) = 0.1\%$ ). A logarithmic scale on the time axis is used to highlight the initial value of the effective  $\zeta$ -potential.

of network formation is in qualitative agreement with the conductivity results. From the CFM image of a typical particle network (Figure 1b) it can be clearly observed that self-similar coherent structures are formed in the sample section that is available through this technique (it should be noted that Figure 1b is representative in terms of topology but not necessarily in terms of particle density). Bigger fractal clusters that partly contain denser agglomerates of particles are formed after a longer time period. The appearance of mainly fractal networks as shown in Figure 1b (starting from widely homogeneous dispersions) and the time evolution of the conductivity suggest mainly diffusion-limited aggregation kinetics in these systems.<sup>25</sup>

A simple but reliable argument that the ion conductivity is due to network formation is supplied by Figure 2a, which shows that ultrasonic treatment leads to a sudden conductivity loss ascribed to network interruption that is followed by a new recovery.

For further verification of the time-dependent agglomeration,  $\zeta$ -potential and DLS measurements were performed. Freshly prepared 0.1 M LiClO<sub>4</sub>/THF/SiO<sub>2</sub> yielded an effective<sup>5</sup> (i.e., semiquantitative)  $\zeta$  potential of  $-62$  mV (Figure 2b). The high value is typical for colloidal solutions<sup>26</sup> and high enough to prevent flocculation and sedimentation. The negative sign indicates a negative surface charge of the particles, which corresponds to anion adsorption and thus explains the increase in Li conductivity. With time, the  $\zeta$  potential decreased significantly, pointing toward particle agglomeration,<sup>23</sup> which is connected with a lower surface charge/density ratio. The decrease continued until a value of around  $-25$  mV was reached after 3000 min. The simplest and most obvious reason for the lowered  $\zeta$  potential is the decrease in local surface charge due to newly formed particle–particle contacts. However, the magnitude of the decrease points toward a more complex situation. The evaluation of the  $\zeta$  potential uses a defined and constant particle radius and does not account for the complex morphology. It lies in the nature of the electroacoustic method that not all of the charges contribute to the effective  $\zeta$  potential measured. It can be assumed that with increased cluster size a greater portion of the “inner surface charge” is overlooked in the electroacoustic measurements. This loss of active surface charge is smaller when the agglomerate decomposes in smaller units, as it is the consequence of coarsening. Thus, not only the pronounced variation of the  $\zeta$  potential finds its explanation in the agglomeration: even the slight decrease in  $\zeta$  potential observed after and before an

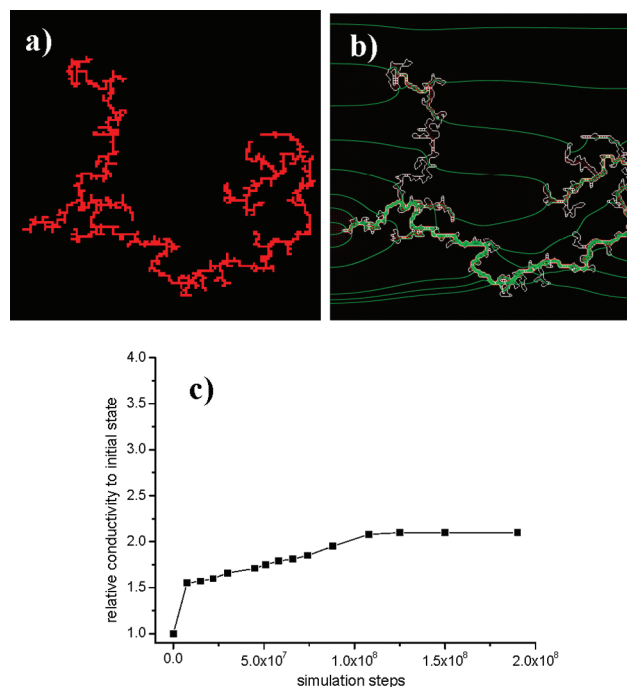


**Figure 3.** (a) Cluster structure from Monte Carlo simulation and (b) current density from subsequent FEM calculation. (c) Relative increase in conductivity for the formed structures during aggregation in comparison with the initial state at  $t = 0$ . The final  $\sigma/\sigma_0$  ratio was 2.1.

agglomeration step may be explained by the superimposed coarsening, emphasizing the inhomogeneous nature of the dispersions. It is tempting to attribute the steps in the  $\zeta$  potential to agglomeration steps. Whether this is really the case has to be investigated in the future.

DLS also indicates agglomeration (Figure S3), in good agreement with the corresponding conductivity data. In spite of the pronounced scatter, the data suggest that particles initially in a homogeneous and well-dispersed state agglomerate as time elapses. This process becomes flattened after several thousand minutes, in rough agreement with the plateau in the  $\sigma$  measurements. The results show a strong variation of the cluster size, corresponding to the highly dynamic processes during cluster formation and deformation. The time-dependent developments of the particle size measured with help of DLS as well as the conductivity behavior indicate a diffusion-limited aggregation process. More detailed mechanistic considerations are beyond the scope of the present paper.

As the bulk electrolyte conductivity (corresponding to the filler-free electrolyte) is not negligible, the overall conductivity evolution of a composite electrolyte is a complex function of time and is only accessible numerically. Figure 3 shows the time dependence of the conductivity modeled using Monte Carlo simulations plus FEM. The morphological network structure was modeled by Monte Carlo simulations as described in simplified terms in ref 6, while FEM was used to compute the corresponding current density distribution.

Figure 3a shows a typical cluster obtained by Monte Carlo simulations using very low oxide particle volume fractions on a two-dimensional (2D) lattice. It was analyzed with respect to current density distribution using FEM. Even though 2D modeling was used, there is a qualitative agreement between modeling and experiment with respect to an increased conductivity in



comparison with the initial state. Unlike the starting situation of a nearly colloidal situation, where only a few small clusters are present because of statistical occupation of lattice sites, the shown image represents an advanced state of the simulation. It is characterized by a single not completely percolating cluster. The calculated current density distribution for such a cluster offered by FEM (COMSOL Multiphysics 4.0a) is presented in Figure 3b, which shows representative current pathways that are influenced by the higher conductivity in the vicinity of the particles. Here the (electrical) flow line density is proportional to the current density (magnitude controlled). For simplicity's sake, both the conductivity and thickness of the surface layer were chosen in a simplified way. The layer thickness is just identified with the pixel size, and the conductivity of the layer is assumed to be constant with a value chosen to be 200 times the bulk conductivity, close to the estimation in ref 27. The conductivity modeling is aggravated by the fact that the conductivity of the SiO<sub>2</sub>-free electrolyte is by no means negligible, as also seen in Figure 3b. Hence, a conductivity increase is continuously observed even below the percolation threshold with increasing proportion of interfacial conductivity (see the current lines that lead through the electrolyte).

In the simulations, the maximum ratio of the final and initial conductivities was  $\sim 2.1$ . This value is a little less than in the experiment but reasonable in view of the 2D modeling and the underlying simplicity. The progress of the change of  $\sigma$  upon agglomeration is displayed in Figure 3c. We actually do not expect a quantitative mapping of our experimental results, but what we clearly see is the characteristic tendency to obtain more-or-less linear subparts, which we characteristically observed in the experiments (Figure 1a).

Freshly prepared composite liquid electrolytes with very low volume fractions of SiO<sub>2</sub> particles show a conductivity increase with time that reflects the slow formation of SiO<sub>2</sub> networks, which finally lead to percolation of highly conducting interfaces. The results are supported by time-dependent effective  $\zeta$ -potential measurements, DLS, and CFM. Most importantly in our contribution, the network formation was recorded in situ using ionic conductivity measurements. The kinetic behavior was semiquantitatively modeled using Monte Carlo simulations in combination with FEM calculations. Beyond the applicability of such systems as electrolytes in Li-based batteries, these investigations give very worthwhile insight into the formation of oxide networks, which is of high significance for various fields of science.

## ■ ASSOCIATED CONTENT

**S** Supporting Information. SEM measurement of SiO<sub>2</sub> particle diameter, Nyquist diagram, and DLS results. This material is available free of charge via the Internet at <http://pubs.acs.org>.

## ■ AUTHOR INFORMATION

**Corresponding Author**  
s.weiglein@fkf.mpg.de

## ■ ACKNOWLEDGMENT

The authors thank Dominik Samuelis for useful discussions.

## ■ REFERENCES

- (1) Martorano, R.; Mattei, I. V.; Johnson, E. A. *J. Coat. Technol.* **1991**, 63, 39.
- (2) Zhang, H. Y.; Xu, F.; Ho, D.; Ilavsky, J.; Justics, M.; Petrache, H.; Stanciu, L.; Xie, J. *ECS Trans.* **2010**, 33, 1335.
- (3) Wiczczonek, W.; Florjanczyk, Z.; Stevens, J. R. *Electrochim. Acta* **1995**, 40, 2251.
- (4) Bhattacharyya, A. J.; Maier, J. *Adv. Mater.* **2004**, 16, 811.
- (5) Jarosik, A.; Hore, S.; Kaskhedikar, N.; Pfaffenhuber, C.; Maier, J. *Electrochim. Acta*, in press; DOI: 10.1016/j.electacta.2011.05.063.
- (6) Jarosik, A.; Traub, U.; Bunde, A.; Maier, J. *Phys. Chem. Chem. Phys.* **2010**, 13, 2663.
- (7) Das, S.; Bhattacharyya, A. J. *J. Phys. Chem. C* **2009**, 113, 6699.
- (8) There are various conductivity studies in the context of solid-solid dispersions. For example, see: Maier, J. *Prog. Solid State Chem.* **1995**, 23, 171. Zavyalov, S. A.; Pivkina, A. N.; Schoonman, J. *Solid State Ionics* **2002**, 147, 415. However, these refer to frozen-in structures that are not comparable with the problem described here.
- (9) Bunde, A.; Dieterich, W.; Roman, H. E. *Phys. Rev. Lett.* **1985**, 55, 5.
- (10) Jarosik, A.; Pfaffenhuber, C.; Bunde, A.; Maier, J. *Adv. Funct. Mater.*, in press; DOI: 10.1002/adfm.201100351.
- (11) Prasad, V.; Semwogerere, D.; Weeks, E. R. *J. Phys.: Condens. Matter* **2007**, 19, No. 113102.
- (12) Lu, P. J.; Conrad, J. C.; Wyss, H. M.; Schofield, A. B.; Weitz, D. A. *Phys. Rev. Lett.* **2006**, 96, No. 028306.
- (13) de Hoog, E. H. A.; Kegel, W. K.; van Blaaderen, A.; Lekkerkerker, H. N. W. *Phys. Rev. E* **2001**, 64, No. 021407.
- (14) Verhaegh, N. A. M.; van Blaaderen, A. *Langmuir* **1994**, 10, 1427.
- (15) Weitz, D. A.; Oliveria, M. *Phys. Rev. Lett.* **1984**, 52, 1433.
- (16) Chen, K. L.; Mylon, S. E.; Elimelech, M. *Environ. Sci. Technol.* **2006**, 40, 1516.
- (17) Lu, P. J.; Zaccarelli, E.; Ciulla, F.; Schofield, A. B.; Sciortino, F.; Weitz, D. A. *Nature* **2008**, 453, 499.
- (18) Bele, M.; Siiman, O.; Matijevic, E. *J. Colloid Interface Sci.* **2002**, 254, 274.
- (19) Haw, M. D.; Sievwright, M.; Poon, W. C. K.; Pusey, P. N. *Adv. Colloid Interface Sci.* **1995**, 62, 1.
- (20) Hatlo, M. M.; Lue, L. *Soft Matter* **2008**, 4, 1582.
- (21) Fornés, J. A. *Colloid Polym. Sci.* **1985**, 263, 1004.
- (22) Sauer, S.; Löwen, H. *J. Phys.: Condens. Matter* **1996**, 8, L803.
- (23) Shilov, V. N.; Borkovskaja, Y. B.; Dukhin, A. S. *J. Colloid Interface Sci.* **2004**, 277, 347.
- (24) Notari, R.; Abboud, J. L. M. *Pure Appl. Chem.* **1999**, 71, 645.
- (25) Weitz, D. A.; Huang, J. S.; Lin, M. Y.; Sung, J. *Phys. Rev. Lett.* **1984**, 53, 1657.
- (26) Dukhin, A. S.; Goetz, J. *Ultrasound for Characterizing Colloids: Particle Sizing, Zeta Potential, Rheology*; Elsevier: Amsterdam, 2002.
- (27) Beyazyildirim, S.; Kreuer, K. D.; Schuster, M.; Bhattacharyya, A. J.; Maier, J. *Adv. Mater.* **2008**, 20, 1274.